# Decolorization of water for domestic supply employing UV radiation and hydrogen peroxide

C.A. Martín, O.M. Alfano, A.E. Cassano*

*Instituto de Desarrollo Tecnológico para la Industria Química (INTEC), Universidad Nacional del Litoral — CONICET, Guemes 3450, 3000 Santa Fe, Argentina*

## Abstract

A kinetic study concerning water decolorization using a combination of low wavelength UV radiation (253.7 nm) and hydrogen peroxide has been performed. Kinetic studies were carried out in a specially designed flat plate reactor, made in such a way that almost "isoactinic" conditions are achieved. Results were analyzed in terms of a very simple kinetics expression. Absorbed radiation effects were duly quantified by means of a one-dimensional radiation field model. With experimental degradation rates, a kinetics expression relating the initial color (expressed in terms of initial total organic carbon) with the most important process variables was proposed and the decolorization kinetics parameters were obtained. The initial decolorization rates at 25°C can be properly represented with an equation of the following form: $R_{TOC}^0 = -kC_{TOC}^0 e^a(z)$. © 2000 Elsevier Science B.V. All rights reserved.

*Keywords:* Water decolorization; UV radiation; Hydrogen peroxide; Photoreactor

## 1. Introduction

Advanced oxidation technologies can be used for treating a large variety of pollutants in air and water. Different processes have been investigated and among them the use of UV radiation has been proposed as a suitable alternative in the past decades [1–3]. In order to improve degradation rates UV radiation alone is not used but combined with strong oxidants such as ozone, hydrogen peroxide, the Fenton reagent or a semiconductor photocatalyst.

Some examples where the oxidative decolorization of wastewater using advanced oxidation processes have been studied, can be found in the papers published by Gregor [4] and Shu and Huang [5]. In [4],

decolorization of textile wastewater was investigated by comparison of three treatment methods: hydrogen peroxide/UV radiation, hydrogen peroxide/ozone, and hydrogen peroxide/Fenton's reagent. The objective of Shu and Huang [5] was to study the decolorization of a wastewater stream using hydrogen peroxide/UV radiation in a well-mixed batch photoreactor. The authors also reported a kinetic model that includes the radiation absorption by the highly colored wastewater.

Sometimes, provision of water for domiciliary consumption faces the problem of natural contamination originated by the presence of organic substances either dissolved or in colloidal state, such as humic or fulvic acids. Very often, after conventional sanitary treatments this water exhibits a persistent yellowish coloration that affects its use, particularly for drinking purposes. Moreover, in some cases these substances act as precursors of tri-halomethanes that may be formed during pre-desinfection with chlorine [6].

* Corresponding author. Tel.: +54-342-455-9175;
fax: +54-342-455-9185.
*E-mail address:* acassano@alpha.acride.edu.ar (A.E. Cassano)

This much more undesirable contamination can be present — even if in very low concentrations — in the final product.

In this work we report the results of a kinetic study concerning water decolorization using a combination of low wavelength UV radiation (253.7 nm) and hydrogen peroxide.

## 2. Experimental

### 2.1. Set-up

Kinetic studies were performed in a specially designed reactor. The reactor was made in such a way that almost "isoactinic" conditions are achieved. This means that spatial variations of the radiation field, for the whole reactor volume, are less significant. With this purpose, a flat plate reactor of circular cross section was irradiated from both sides with two tubular lamps placed at the focal axis of two parabolic reflectors made of an aluminum sheet, mirror polished, with Alzac treatment (Fig. 1).

The reactor was made of Pyrex glass while irradiated windows were made of Suprasil quartz. The reactor was placed inside a recycling system having a storage tank and a recirculating pump (Masterflex model 7518-12). The whole system operated in the batch mode. Incident radiation was varied in three different levels: (i) Philips TUV lamp (15 W), (ii)
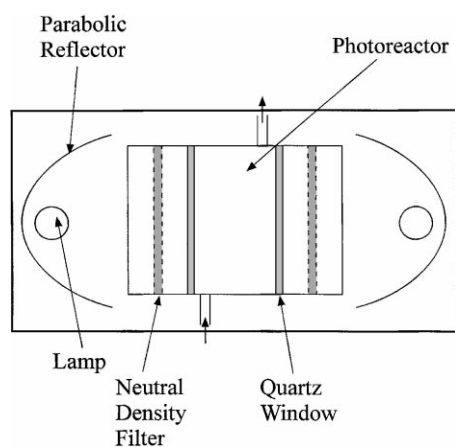


Fig. 1. Flat plate photoreactor of circular cross section.

Table 1
Experimental set-up

|  | Parameter | Value |
| --- | --- | --- |
| Reactor |  |  |
|  Pyrex | Diameter (cm) | 4.4 |
|  Suprasil | Length (cm) | 4.9 |
|  | Volume (cm$^3$) | 74.5 |
| Lamps |  |  |
|  Heraeus UV–C NNI 40/20 (253.7 nm) | Input power (W) | 40 |
|  | Output power (W) | 12 |
|  Philips TUV 15 (253.7 nm) | Input power (W) | 15 |
|  | Output power (W) | 3.5 |
| Reservoir | Volume (cm$^3$) | 1000 |

Heraeus UV–C lamp (40 W), and (iii) Heraeus UV–C lamp with a neutral density filter. An all glass heat exchanger connected to a thermostatic bath permitted temperature control, and the lamps operation was monitored with VAW meter (Clarke Hess, model 255).

Further details and characteristics of the employed experimental set-up are described in Table 1 and Fig. 2.

### 2.2. Procedure

Three experimental variables were investigated: (1) the initial color of the water to be treated, (2) the hydrogen peroxide concentration (Carlo Erba RPE-ACS 30%), and (3) the volumetric rate of energy absorption (VREA). The main body of all experiments was conducted at pH = 3.5 and temperature of 25°C.

The organic compound concentration in water was followed with total organic carbon (TOC) measurements (Shimadzu TOC-5000A) and hydrogen peroxide was analyzed with spectrophotometric methods [7] (UV–Vis Cary 17 D Spectrophotometer). Additional experimental information was also collected: (1) the optical characteristics (absorbance) of the reacting mixture was controlled in all samples and (2) at the start and the end of representative runs, the color of the mixture was measured with the Visual Comparison Method [8].

The water color index could be correlated with the total organic concentration, as it is shown in Fig. 3. Hence, we can obtain the color index variation by means of a more convenient analytical variable: the TOC content.
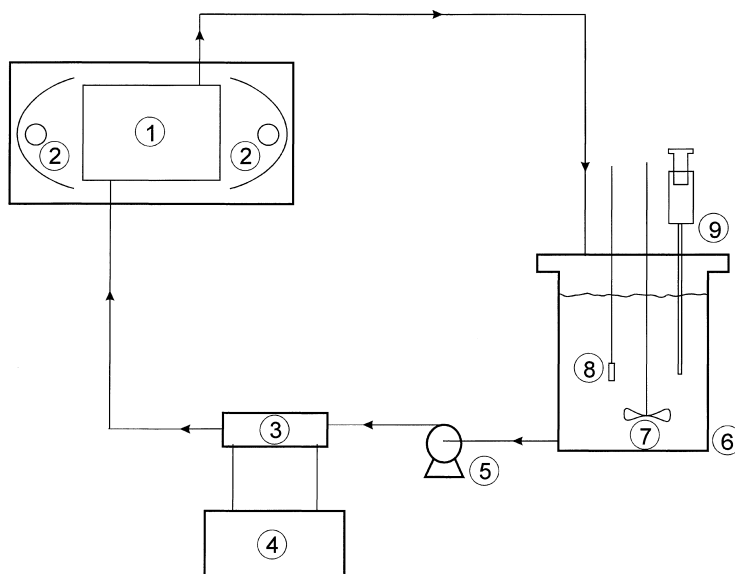
Fig. 2. Experimental set-up. (1) Photoreactor, (2) lamps, (3) heat exchanger, (4) thermostatic bath, (5) pump, (6) tank, (7) stirrer, (8) thermometer, and (9) sampling port.

The water, coming from rivers in the northern part of Argentina, was filtered (Micronsep, Cellulosic, Sterile, 0.45 μ) and the pH adjusted with the addition of sulfuric acid.

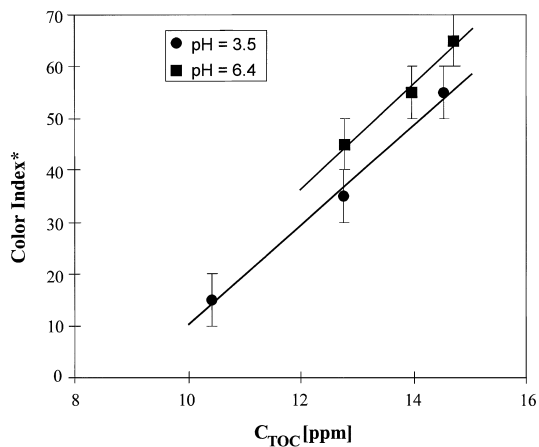Prior to any experimental run, reactor temperature and lamp operation were monitored during 1–2 h; during this time a shutter was interposed between the lamps and the reactor. Once steady-state conditions were achieved the desired amount of hydrogen peroxide was added to the mixture and mechanical stirring mixed the reacting system. The removal of the shutters indicated the zero reaction time.

Samples ($30 \, \text{cm}^3$) were taken from the tank at specific time intervals (1 h) for the different analysis. Table 2 shows operating conditions for the experimental program.

Table 2
Experimental program

| Variable | Range |
|---|---|
| TOC (ppm) | 2–6 |
| Hydrogen peroxide (ppm) | 50–250 |
| Incident radiation (Einstein $\text{cm}^{-2} \, \text{s}^{-1}) \times 10^9$ | |
|   Heraeus 40 W (100%) | 14.95 |
|   Philips 15 W (39%) | 5.85 |
|   Heraeus 40 W (16%) (with neutral filter) | 2.50 |



Fig. 3. Color index[(*)] vs. TOC concentration. (*) Visual comparison method [8].

## 3. Results

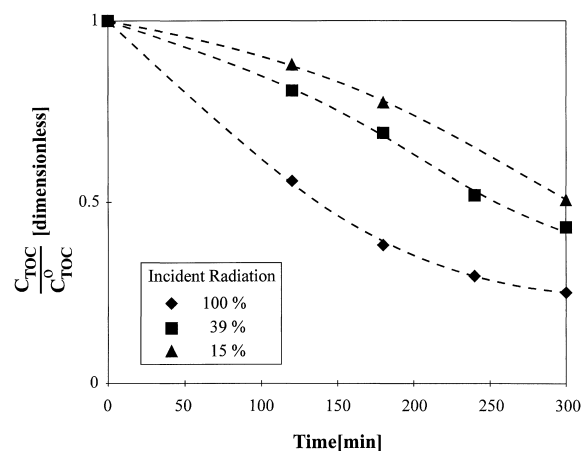Fig. 4 shows the TOC time evolution for three typical runs with different irradiating conditions. It must

Fig. 4. TOC concentration (dimensionless) vs. time for three different irradiating conditions. Incident radiation: relative to Heraeus UV–C NNI 40 W (100%).

be noted that even if the TOC concentration is not zero at the end of the run, water fulfilled international standards for drinking water.

Fig. 5 shows GC–MS results of the untreated and treated water, respectively. We can see a dramatic decrease in the concentration for most of the organic substances analyzed by gas chromatography with a mass spectrometer detector (Shimadzu GCMS QP5000).

## 4. Reactor model

### 4.1. Radiation field

The radiation distribution of the described system can be obtained by solving the radiative transfer equation using a three-dimensional cylindrical coordinate system for the homogeneous medium (no radiation emission inside the reactor):

$$\frac{\mathrm{d}I_{\lambda,\boldsymbol{\Omega}}(s,t)}{\mathrm{d}s} + \kappa_\lambda(s,t)I_{\lambda,\boldsymbol{\Omega}}(s,t) = 0 \tag{1}$$

The parametric representation of the ray trajectory is given by the variable $s$. Eq. (1) is valid for monochromatic light and a single direction $\boldsymbol{\Omega}$. Solution of this differential equation provides the field of radiation intensities. However, the relevant photochemical prop-

erty, for the material point located at $\mathbf{x}$, is the spectral incident radiation [9]:

$$G_\lambda(\mathbf{x},t) = \int_\Omega I_{\lambda,\boldsymbol{\Omega}}(\mathbf{x},t)\,\mathrm{d}\Omega \tag{2}$$

In Eq. (2) an integration over the solid angle $\Omega$ for all possible directions proceeding from the emitting system has been effected.

In a previous paper, Alfano et al. [10] proposed a rigorous radiation field model generated by a tubular UV lamp and a cylindrical reflector of parabolic cross section. The model was experimentally verified with variable spatial position microreactors [11,12] and it was found that, for specific geometric arrangements, radial and angular variations were not significant. This particular system is a good approximation to such an ideal system and hence the radiation field for monochromatic lamp emission ($\lambda=253.7$ nm) can be described with a one-dimensional model. In this case, the equation for the spectral incident radiation takes the following form:

$$\frac{\mathrm{d}G_\lambda(z,t)}{\mathrm{d}z} + \kappa_\lambda(z,t)G_\lambda(z,t) = 0 \tag{3}$$

The incident radiation at a given point $z$, can be obtained from a very simple expression

$$G(z,t) = G_\mathrm{w}\exp[-\kappa_\mathrm{T}(t)z] \tag{4}$$

where $G_\mathrm{w}$ is the incident radiation at the reactor wall and $\kappa_\mathrm{T}$ is the total absorption coefficient of the reacting system (reactants, products, inerts, etc.). Clearly, $\kappa_\mathrm{T}$ is a function of time.

In the case of our isoactinic reactor, radiation originated in lamps I and II, may arrive at any point $P$ from two opposite sides (see Fig. 6). Then,

$$G_\mathrm{T}(z,t) = G_\mathrm{I}(z,t) + G_\mathrm{II}(z,t) \tag{5}$$

with

$$G_\mathrm{I}(z,t) = G_\mathrm{w,I}\exp[-\kappa_\mathrm{T}(t)z],$$
$$G_\mathrm{II}(z,t) = G_\mathrm{w,II}\exp[-\kappa_\mathrm{T}(t)(L_\mathrm{R} - z)] \tag{6}$$

The local volumetric rate of radiation energy absorption for reaction of species R, at a given point $P$ (the LVREA) is given as follows:

$$e^\mathrm{a}(z,t) = \kappa_\mathrm{R}(t)G_\mathrm{T}(z,t) \tag{7}$$
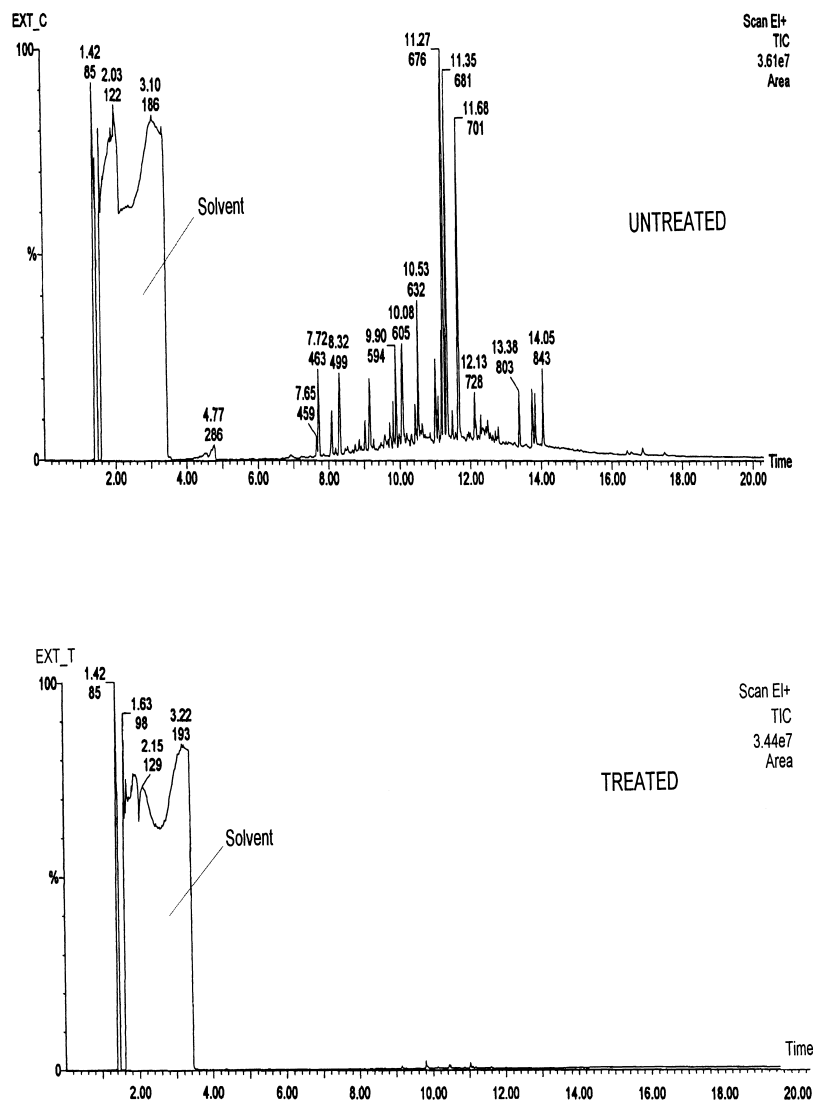
Fig. 5. GC–MS of untreated and treated water. $H_2O_2$: 150 ppm, germicidal lamp: 15 W, total run time: 10 h.

where $\kappa_R$ is the volumetric absorption coefficient of the reacting species R. Volumetric absorption coefficients can be obtained from direct application of Beer's equation (e.g., for the decoloration reaction, $\kappa_R = C_{H_2O_2} \times \kappa^*_{H_2O_2}$).

If $G_{w,I}=G_{w,II}=G_w$, substituting Eq. (6) into Eq. (5), and the resulting equation into Eq. (7), gives:

$$e^a(z, t) = \kappa_R(t)G_w\{\exp[-\kappa_T(t)z] + \exp[-\kappa_T(t)(L_R - z)]\} \qquad (8)$$

### 4.2. Mass balance

Both, the reactor and the tank, operate under perfect mixing conditions and constant temperature. The lamp operation is also constant. According to Martín et al. [13], concentration changes of the reacting species ($i$) inside the batch recycling system are obtained from the following mass balance:

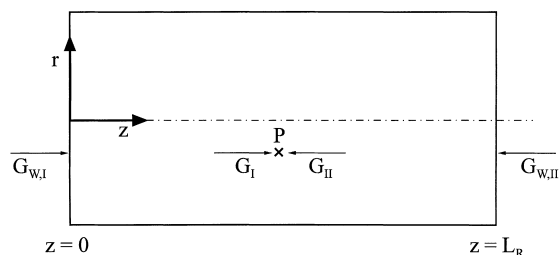$$\frac{dC_i(t)}{dt} = \frac{V_R}{V_T}\langle R_i(z, t)\rangle_{V_R} \qquad (9)$$

Fig. 6. Incident radiation at a given point of the isoactinic reactor. $G_I$: primary beam, $G_{II}$: secondary beam, $G_w$: incident radiation at the reactor wall (boundary condition).

with the initial condition

$$C_i(t=0) = C_i^0 \qquad (10)$$

This equation is valid when: (1) $V_R/V_T \ll 1$, (2) the storage tank is perfectly stirred, and (3) there is no chemical reaction inside the tank.

### 4.2.1. The boundary condition: actinometry

Incident radiation at $z=0$ and $z=L_R$ can be evaluated with actinometer measurements employing, e.g., potassium ferrioxalate. For the actinometer reaction, with $i=P$

$$R_A(z,t) = -R_P(z,t) = -\Phi_P e^a(z,t) \qquad (11)$$

In the above equation A is the reactant ($Fe^{3+}$), P the reaction product ($Fe^{2+}$) and $\Phi_P$ the overall quantum yield.

In the described reactor, for low reactant ($Fe^{+3}$) conversion, the plot of ($Fe^{2+}$) vs. time gives a straight line. The slope of such line at $t \to 0$ is

$$\left(\frac{dC_P}{dt}\right)_{t \to 0} = \lim_{t \to 0}\left(\frac{C_{Fe^{2+}} - C_{Fe^{2+}}^0}{t - t^0}\right) \qquad (12)$$

Using Eqs. (8), (9), (11) and (12), integrating in the reactor volume, and considering that at the initial conditions: (i) $\kappa_P(t \to 0) \cong 0$ and (ii) at 253.7 nm $\kappa_A$ for this actinometer is very large, we can obtain [14]

$$G_{w,I} = G_{w,II} = G_w$$
$$= \lim_{t \to 0}\left(\frac{C_{Fe^{2+}} - C_{Fe^{2+}}^0}{t - t^0}\right)\frac{V_T}{A_R \Phi_P} \qquad (13)$$

In Eq. (13) $A_R$ is the total area of radiation entrance (the sum of the two quartz windows).

### 4.2.2. Water decolorization

The reactor for treating the colored water also operates under the conditions described above. Hence, the water decolorization mass balance gives

$$\frac{dC_{TOC}(t)}{dt} = \frac{V_R}{V_T}\langle R_{TOC}(z,t)\rangle_{V_R} \qquad (14)$$

with

$$C_{TOC}(t=0) = C_{TOC}^0 \qquad (15)$$

In a kinetically controlled photochemical reaction, whichever is the mechanism, the local initiation rate is always some function of the LVREA. Since the LVREA is a function of the spatial coordinates, the same dependence is translated into the reaction rate. Considering that radial and angular variations are not significant, $R_{TOC}$ becomes a function of only $z$ and $t$.

In Eq. (14) an average reaction rate has been defined according to

$$\langle R_{TOC}(z,t)\rangle_{V_R} = \langle R_{TOC}(z,t)\rangle_{L_R}$$
$$= \frac{1}{L_R}\int_0^{L_R} R_{TOC}(z,t)\,dz \qquad (16)$$

For this reacting system, a mechanistically derived kinetic expression is not possible. However, at constant pH and considering the most relevant variables, one can propose a phenomenological expression to represent the evolution of the TOC concentration. Then, in mathematical terms, we are seeking for an expression of the following form:

$$R_{TOC}(\mathbf{x},t) = \Im[C_{TOC}(\mathbf{x},t), C_{H_2O_2}(\mathbf{x},t), e^a(\mathbf{x},t)] \qquad (17)$$

The specific form of the function $\Im$ will be defined by experiments.

## 5. Results

### 5.1. Boundary conditions ($G_w$)

Fig. 7 shows the experimental results of the actinometric runs. The plot represents the $Fe^{2+}$ concentration vs. time for three different irradiating conditions. From the slope, according to Eq. (13) we can obtain the boundary conditions for the three irradiation levels. The results are shown in Tables 1 and 2.
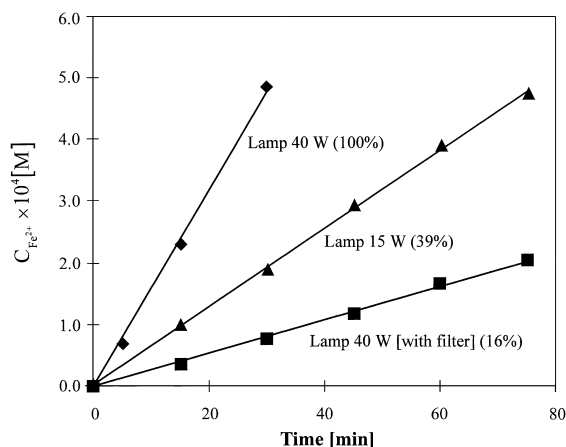
Fig. 7. Actinometric measurements. Actinometer: potassium ferrioxalate 0.006 M.

### 5.2. Kinetic parameter evaluation

With the set of experimental decolorization data, we are now in a position to obtain the kinetic parameters. Let us propose the following simple relationship:

$$R_{TOC}(z, t) = k[C_{TOC}(t)]^m [C_{H_2O_2}(t)]^n [e^a(z, t)]^p \quad (18)$$

where the independent variables are: (i) TOC, (ii) hydrogen peroxide concentration, and (iii) LVREA. Notice, however, that from Eqs. (4) and (7) the LVREA depends on the hydrogen peroxide concentration in a linear form and on the reactants and products concentration in an exponential form.

Since the reactor is well mixed, the average values at initial conditions are:

$$\langle C_{TOC}(t \to 0) \rangle_{V_R} = C_{TOC}^0 \quad (19)$$

$$\langle C_{H_2O_2}(t \to 0) \rangle_{V_R} = C_{H_2O_2}^0 \quad (20)$$

$$\langle R_{TOC}(z, t \to 0) \rangle_{V_R} = \langle R_{TOC}^0(z) \rangle_{L_R} = R_{TOC}^0 \quad (21)$$

$$\langle e^a(z, t \to 0) \rangle_{L_R}$$
$$= \frac{1}{L_R} \int_0^{L_R} \kappa_{H_2O_2}(t \to 0) G_w \{ \exp[-\kappa_T(t \to 0)z]$$
$$+ \exp[-\kappa_T(t \to 0)(L_R - z)] \} \, dz \quad (22)$$

where $\kappa_{H_2O_2} = \kappa_{H_2O_2}(t) = \kappa_{H_2O_2}^* C_{H_2O_2}(t)$ is the hydrogen peroxide absorption coefficient and $\kappa_T = \kappa_T(t)$

because the concentration of reactants and products is also changing with time.

Using Eqs. (14) and (18)–(22) the volume average reaction rate at $t \to 0$ is given by:

$$R_{TOC}^0 = k(C_{TOC}^0)^m (C_{H_2O_2}^0)^n \frac{1}{L_R} \int_0^{L_R}$$
$$\{ \kappa_{H_2O_2}^0 G_w \{ \exp(-\kappa_T^0 z)$$
$$+ \exp[-\kappa_T^0(L_R - z)] \} \}^p \, dz \quad (23)$$

For an ideal, isoactinic reactor:

$$\frac{1}{L_R} \int_0^{L_R} \{ \kappa_{H_2O_2}^0 G_w \{ \exp(-\kappa_T^0 z)$$
$$+ \exp[-\kappa_T^0(L_R - z)] \} \}^p \, dz$$
$$\cong \left\{ \frac{1}{L_R} \int_0^{L_R} \kappa_{H_2O_2}^0 G_w \{ \exp(-\kappa_T^0 z)$$
$$+ \exp[-\kappa_T^0(L_R - z)] \} \, dz \right\}^p \quad (24)$$

Our reactor that is irradiated from both sides and employs low hydrogen peroxide concentrations approaches the isoactinic behavior. Then,

$$R_{TOC}^0 = k(C_{TOC}^0)^m (C_{H_2O_2}^0)^n$$
$$\left\{ G_w \frac{2\kappa_{H_2O_2}^0}{L_R \kappa_T^0} [1 - \exp(-\kappa_T^0 L_R)] \right\}^p \quad (25)$$

In Eq. (25) we have four unknowns: the kinetic constant $k$, and the exponents $m$, $n$, and $p$.

To obtain the kinetic parameters the following sequence was followed:

1. The experimental data of TOC vs. time were fitted with polynomial regressions to obtain the values of the initial experimental reaction rate $[R_{TOC}^0(\text{Exp.})]$ for each run.
2. The whole set of data from the different runs was fed to a multiparameter, non-linear regression algorithm that is coupled with and optimization program according to the Levenberg–Marquardt method [15]. The regression program gave the values $m=1$, $n=0$, $p=1$, and $k=2.235 \times 10^5$ cm$^3$ Einstein$^{-1}$.
3. With these values we can obtain predicted initial reaction rates $[R_{TOC}^0(\text{Pred.})]$ and compare the results with the experimental ones.

Table 3
Experimental and predicted reaction rate at $t \to 0$

| $C_{TOC}^0$ (ppm) | $C_{H_2O_2}^0$ (ppm) | $G_w \times 10^9$ (Einstein cm$^{-2}$ s$^{-1}$) | $R_{Exp.}^0 \times 10^3$ (ppm s$^{-1}$) | $R_{Pred.}^0 \times 10^3$ (ppm s$^{-1}$) | Error (%) |
|---|---|---|---|---|---|
| 5.17 | 150 | 14.95 | 3.93 | 3.22 | 17.98 |
| 3.96 | 150 | 14.95 | 3.24 | 2.77 | 14.43 |
| 2.37 | 150 | 14.95 | 1.72 | 1.74 | −1.18 |
| 4.43 | 250 | 14.95 | 3.80 | 3.80 | −0.09 |
| 4.71 | 50 | 14.95 | 1.30 | 1.18 | 9.00 |
| 3.81 | 150 | 2.50 | 0.50 | 0.42 | 15.53 |
| 4.09 | 150 | 5.85 | 0.88 | 1.04 | −18.73 |

Table 3 shows some operating conditions and the obtained results. For the whole experimental program, deviations between predictions [$R_{TOC}^0$(Pred.)] and experimental data [$R_{TOC}^0$(Exp.)] were never greater than 18.7%.

Finally, the kinetic expression for the decolorization of water is obtained

$$R_{TOC}^0 = -2.235 \times 10^5 (C_{TOC}^0) \langle [e^a(z)] \rangle_{L_R} \qquad (26)$$

These results should not be interpreted as zero-order dependence with respect to hydrogen peroxide concentration. From Eq. (22) it can be seen that the LVREA bears a direct linear dependence with the hydrogen peroxide concentration. The hydrogen peroxide concentration is also a part of the total absorption coefficient that affects the negative exponential function.

## 6. Conclusions

- A kinetic study concerning water decolorization for domestic supplies has been performed. The experimental study was carried out in a flat plate photoreactor of circular cross section (with almost isoactinic performance). It was irradiated from both sides with two tubular, germicidal lamps placed at the focal axis of two cylindrical reflectors of parabolic cross section.
- For this water decolorization process, the relationship: color index (with Standard Methods) vs. TOC was established.
- By comparison of untreated and treated water, a significant decrease in the concentration of most of the organic substances that were initially present was found.

- The water decolorization kinetics was modeled with initial reaction rates obtained from TOC vs. time measurements. At constant pH (3.5), three experimental variables were investigated: (i) initial TOC concentration of the water to be treated, (ii) hydrogen peroxide concentration, and (iii) incident radiation at the wall of the radiation entrance.
- A very simple kinetic model has been developed to describe the water decolorization process using UV and hydrogen peroxide. The model parameters were obtained from experimental data.

## Acknowledgements

## References

[1] D.F. Ollis, H. Al-Ekabi (Eds.), Photocatalytic Purification and Treatment of Water and Air, Elsevier, Amsterdam, 1993.
[2] O. Legrini, E. Oliveros, A.M. Braun, Chem. Rev. 93 (1993) 671.
[3] Abstracts from the Proceedings of the Fifth International Conference on Advanced Oxidation Technologies for Water and Air Remediation, Albuquerque, May 24–28, 1999.
[4] K.H. Gregor, in: W.W. Eckenfelder, A.R. Browers, J.A. Roth (Eds.), Chemical Oxidation. Technologies for the Nineties, Vol. 2, Technomic Publishers, Lancaster, Pennsylvania 1994, p. 161.

[5] H.Y. Shu, C.R. Huang, in: Proceedings of the Third International Conference on Advanced Oxidation Technologies for Water and Air Remediation, Cincinnati, October 26–29, 1996.

[6] M.A. Callahan, M. Slimak, N. Gbel, Report EPA-40014-74-029 a,b (1979).

[7] A.O. Allen, C.J. Hochanadel, J.A. Ghormley, T.W. Davis, J. Phys. Chem. 56 (1952) 575.

[8] A.D. Eaton, L.S. Clesceri, A.E. Greenberg (Eds.), Standard Methods for the Examination of Water and Wastewater, 19th Edition, American Public Health Association Washington, DC, 1995, p. 2-2.

[9] A.E. Cassano, C.A. Martín, R.J. Brandi, O.M. Alfano, Ind. Eng. Chem. Res. 34 (1995) 2155.

[10] O.M. Alfano, R.L. Romero, A.E. Cassano, Chem. Eng. Sci. 40 (1985) 2119.

[11] O.M. Alfano, R.L. Romero, A.E. Cassano, Chem. Eng. Sci. 41 (1986) 1155.

[12] O.M. Alfano, R.L. Romero, C.A. Negro, A.E. Cassano, Chem. Eng. Sci. 41 (1986) 1163.

[13] C.A. Martín, M.A. Baltanás, A.E. Cassano, J. Photochem. Photobiol. A 94 (1996) 173.

[14] M.I. Cabrera, C.A. Martín, O.M. Alfano, A.E. Cassano, Wat. Sci. Tech. 35 (1997) 31.

[15] W. Press, W. Vetterling, S.A. Teukolsky, B.P. Flannery, Numerical Recipes in Fortran 77, Vol. 1, 2nd Edition, Cambridge University Press, Cambridge, MA, 1996, p. 678 (Chapter 15).